Laser-Heated Flashlamps: a Step Toward a Soft X-Ray Laser

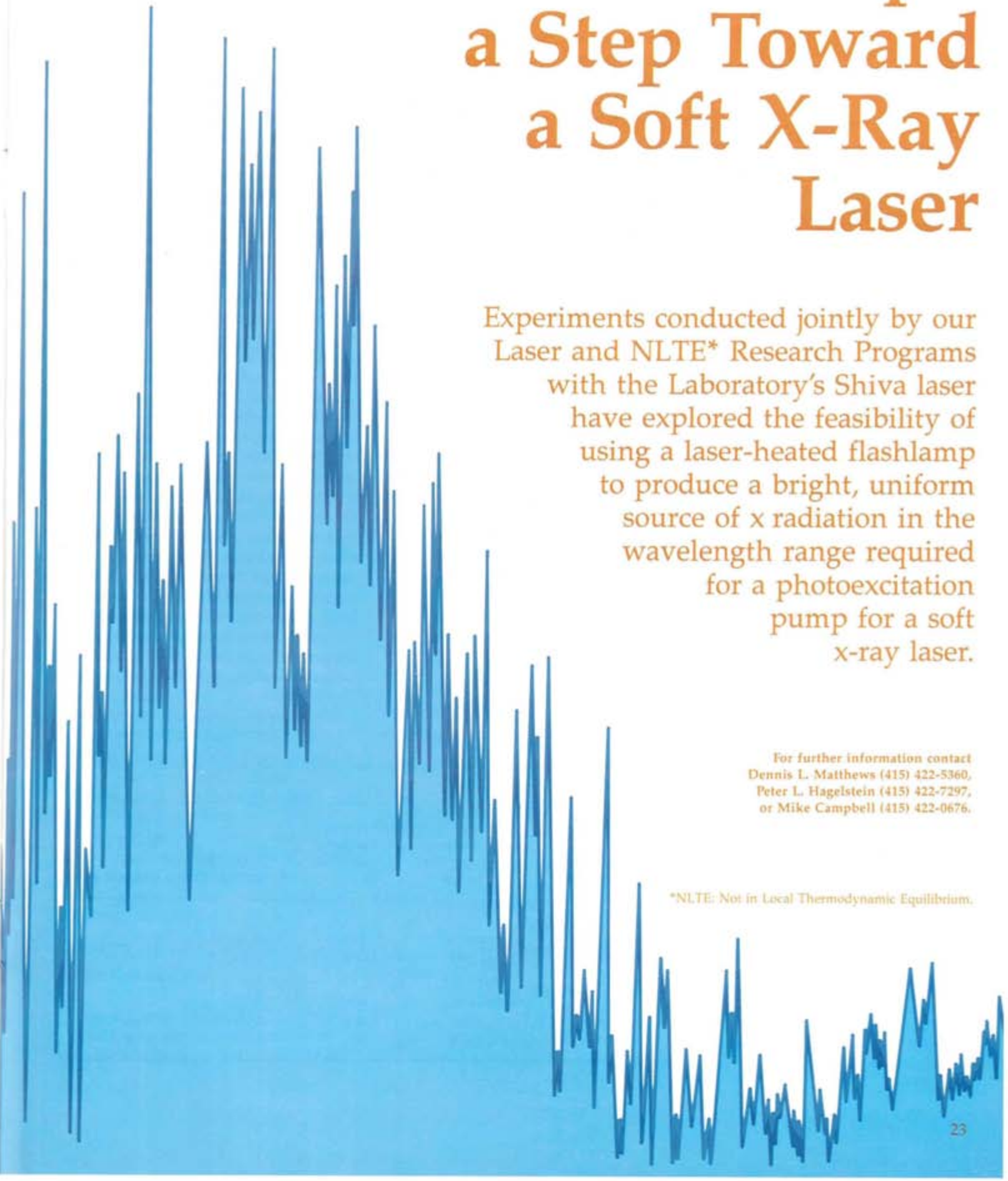

Experiments conducted jointly by our Laser and NLTE* Research Programs with the Laboratory's Shiva laser have explored the feasibility of using a laser-heated flashlamp to produce a bright, uniform source of x radiation in the wavelength range required for a photoexcitation pump for a soft x-ray laser.

For further information contact Dennis L. Matthews (415) 422-5360, Peter L. Hagelstein (415) 422-7297, or Mike Campbell (415) 422-0676.

*NLTE: Not in Local Thermodynamic Equilibrium.

Lasing at x-ray wavelengths has long been pursued both as a challenging technical achievement and as an extremely fruitful extension of the already prolific uses of the optical laser. Applications range from the holography of deoxyribonucleic acid (DNA) molecules to x-ray lithography of microcircuits. As the brightest (i.e., most energetic) available source of coherent radiation, an x-ray laser also would be adaptable to photoelectron spectroscopy and phase-contrast microscopy.

The realization of an x-ray laser poses a complex technical challenge. This is primarily due to the lack of efficient large-angle mirrors from which to form a laser cavity. This results in the apparent need to use dipole transitions to achieve high enough gains to produce significant laser action during a single pass through the laser material. The power needed to pump such dipole transitions scales as the inverse cube of the laser wavelength.

Several investigators have proposed various soft-x-ray lasing schemes using a neodymium-glass laser as the driving source. In the most promising,[1] the driving laser light is used to heat a flashlamp foil (Fig. 1). Upon ionization to a lower state, the foil emits x rays, which are, in turn, used to strip cold neon or fluorine gas down to a helium- or hydrogen-like state of ionization. The resulting ions are resonantly photoexcited by the appropriate x-ray emission line of the flashlamp foil to create a population inversion between either the $n = 4$ and $n = 3$ states or the $n = 3$ and $n = 2$ states (Fig. 2).

In an x-ray laser based on $n = 4 \rightarrow n = 3$ transitions in neon, the x-ray spectrum of the flashlamp foil must contain an emission line near a wavelength of 1.1 nm (within $\pm$ 0.0003 nm) to resonantly photoexcite helium-like ions from their ground state to their $n = 4$ excited state. Electron-ion collisions will then primarily populate states with higher angular momentum [such as the 1s4d(^{1}D), 1s4f(^{1}F) states], which are dipole forbidden to relax to the ground state (see Fig. 2). In addition, the lower state of the x-ray laser—

Fig. 1

In a resonantly pumped x-ray laser, light from a neodymium-glass laser is used to heat a metal flashlamp foil. The foil emits x rays that both ionize and (if the x rays are of the proper wavelength) create a population inversion in a gaseous medium, which lases to produce coherent soft x radiation.

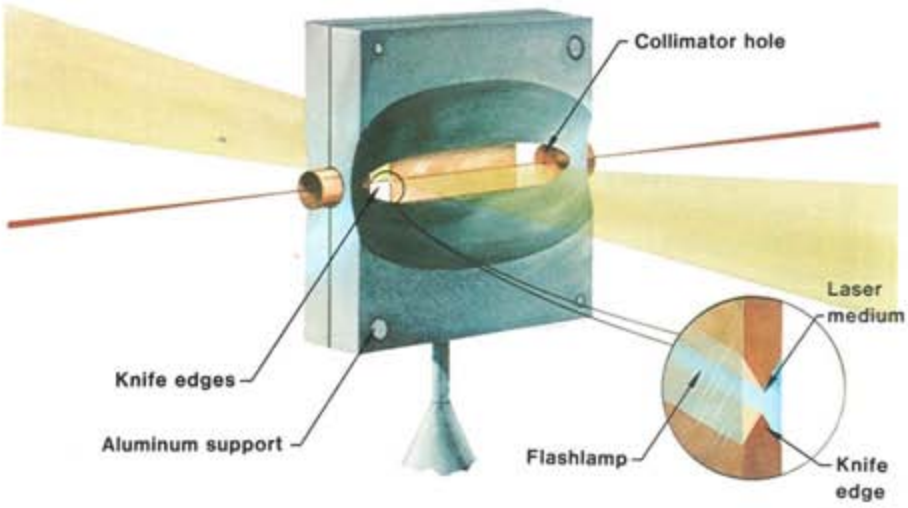

Table 1 Candidate flashlamp materials and lasing media for a resonantly pumped photoexcitation x-ray laser.

Flashlamp material	Measured flashlamp pump line (λ), nm	Required flashlamp pump line (λ), nm	Lasing medium	Energy of lasing medium, eV
$n = 3 \rightarrow n = 2$ schemes				
B-like Cr	1.4458	1.4458	He-like F	119
Be-like Mn	1.2643	1.2643	H-like F	153
$n = 4 \rightarrow n = 3$ schemes				
Be-like Cr	1.3779	1.3782	He-like F	42.3
N-like Ni	1.1000	1.100	He-like Ne	53.6
He-like Na	1.1003	1.100	He-like Ne	53.6

the $1s3p(^1P)$ or $1s3d(^1D)$ state—rapidly decays by dipole emission to the $1s2p(^1P)$ or $1s^2(^1S)$ state. The lasing scheme based on the $n = 3 \rightarrow n = 2$ transition operates similarly, the $n = 3$ state being preferentially excited with a well-chosen flashlamp emission line.

Table 1 summarizes the critical properties of candidate flashlamp materials and lasing media proposed for the photopumped x-ray laser. Except for the helium-like sodium transition, all the pumping-flashlamp foil candidates emit x rays resulting from $n = 3 \rightarrow n = 2$ transitions in ions of moderate atomic number (24 to 28). Although Table 1 is not exhaustive, it represents candidates that have received the closest scrutiny.

X-Ray Lasing Experiments at LLNL

Early in 1983, we will begin a series of experiments to study the feasibility of lasing at x-ray wavelengths. Our technique will use the Laboratory's Novette laser system (which has two arms of the ten-arm Nova laser) to irradiate two thin metal foils with 532-nm laser light. Sandwiched between the foils is a layer of neon gas that serves as the x-ray lasing medium (see Fig. 1). The foils convert the laser light to x rays that are transmitted through the foils to ionize and preferentially excite certain atomic states in the neon gas, which then lases at soft-x-ray wavelengths.

Before we can quantitatively evaluate the proposed scheme, we must know the x-ray emission characteristics of the laser-irradiated flashlamp foils. The last series of experiments performed with the Laboratory's large Shiva laser (before it was dismantled in 1982) was designed primarily to characterize the x-ray emission spectra produced by some of the candidate flashlamp materials.

Design of the Shiva Experiments

Flashlamp Targets

The flashlamp targets consisted of thin metallic foils of iron, iron-copper, chromium, or nickel about 0.04 μm thick and 2 mm in diameter (Fig. 3). The metal was deposited on a 0.5-μm-thick parylene disk that provided mechanical strength; the targets were suspended across a thin (25-μm-thick) Mylar hoop 3 mm in outside diameter. To facilitate centering all of Shiva's ten

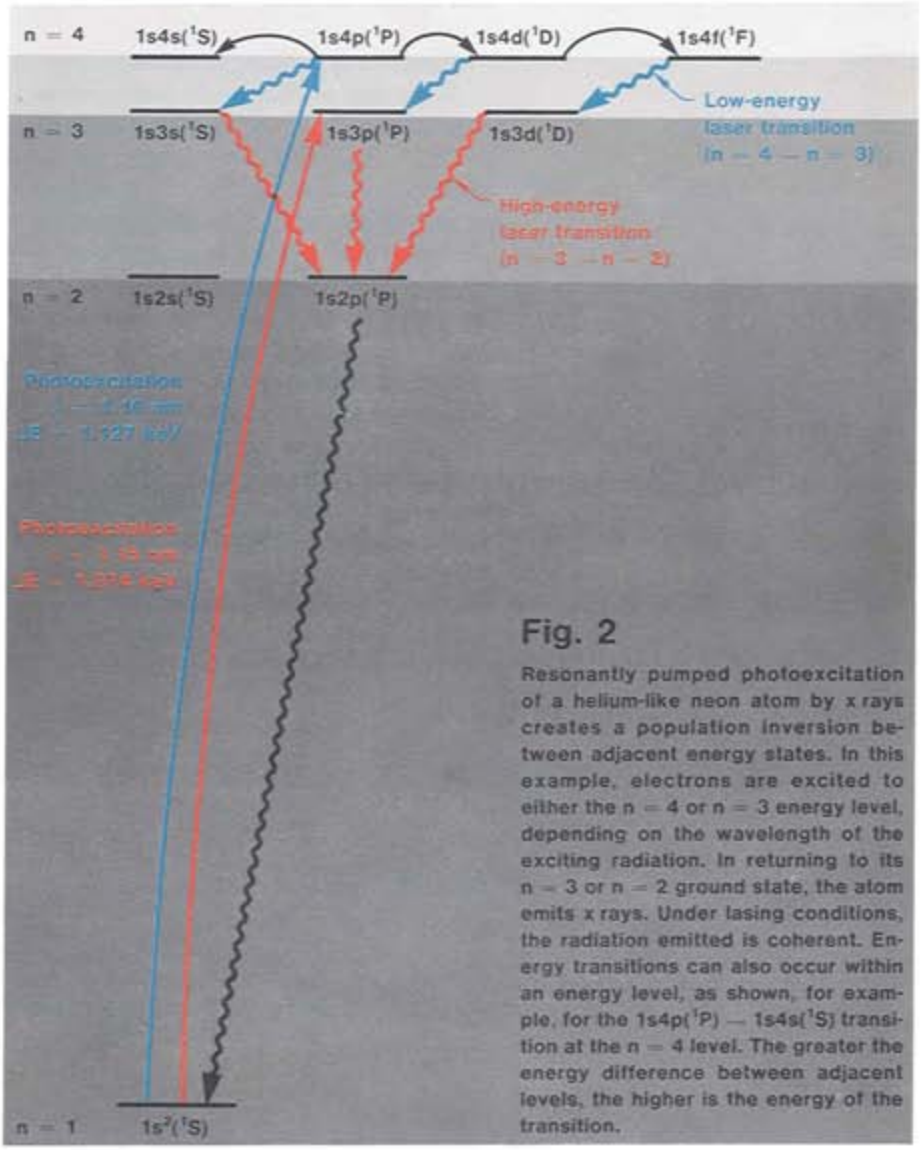

Fig. 2

Resonantly pumped photoexcitation of a helium-like neon atom by x rays creates a population inversion between adjacent energy states. In this example, electrons are excited to either the n = 4 or n = 3 energy level, depending on the wavelength of the exciting radiation. In returning to its n = 3 or n = 2 ground state, the atom emits x rays. Under lasing conditions, the radiation emitted is coherent. Energy transitions can also occur within an energy level, as shown, for example, for the $1s4p(^1P) \rightarrow 1s4s(^1S)$ transition at the n = 4 level. The greater the energy difference between adjacent levels, the higher is the energy of the transition.

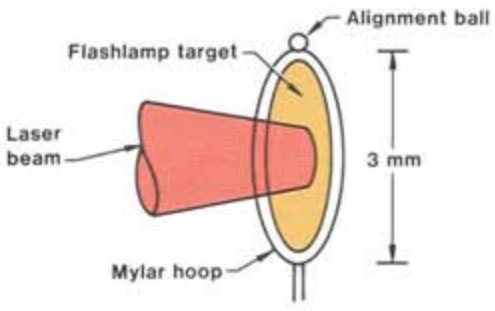

Fig. 3

Typical flashlamp-foil target used in the Shiva x-ray experiments. The metal foil was deposited on a parylene disk to provide mechanical strength. The targets were suspended across a thin Mylar hoop. The ball enabled us to center all of Shiva's ten lower beams on the target.

lower beams, we mounted an alignment ball 300 μm in diameter on each target. To ensure a uniform thickness and composition of the flashlamp targets, we measured the metal foils from which they were cut. The overall uniformity over thickness of about 100 μm (determined by both light transmission and sputter erosion) was at least 20%.

Flashlamp Diagnostics

The array of diagnostic instruments used in the Shiva experiments is shown in Fig. 4. Each flashlamp target was irradiated either normal to the lower set of Shiva's beams for absorption measurements, or rotated at an angle of 30 deg to the normal to enable the diagnostics to view both sides of the target. The primary diagnostic instruments consisted of four crystal spectrographs, which measured the time- and space-integrated x-ray spectra. To obtain information on the angular variation of the x-ray spectrum of the flashlamp foils, we placed two of the spectrographs in front of the flashlamp surface and two at its rear. The rearward spectrographs were of primary importance because they measured the spectrum that will irradiate the lasing medium.[2] Calibrating the response of the film used in the spectrographs to the emitted x rays was a formidable task; it represents the least certain quantity in determining the absolute intensity of the x-ray lines emitted from the flashlamp foils.

The forward spectrographs were set to measure the x-ray emission spectrum from 0.7 to 1.4 keV, the rearward spectrographs from 0.7 to 1.2 keV. To calibrate spectral energy, we placed foils with known absorption characteristics over the entrance apertures of the spectrographs. We also calibrated the spectrographs to known spectral features of the iron and chromium foils. The rearward spectrographs were calibrated to photon energy within $\pm$ 4 eV; the accuracy of their absolute intensity measurements has not yet been determined. The forward spectrographs were calibrated to energy within $\pm$ 5 eV and to absolute intensity within $\pm$ 50%.

The time history (resolved to about 20 ps) of the L-shell emission was measured using a 300-nm-period gold transmission grating, coupled to a soft-x-ray streak camera.[3,4] The spectral resolution of $E/\Delta E = 10$ was, however, insufficient to observe individual emission lines.

We used a polar 8× Kirkpatrick-Baez microscope to measure the uniformity of the time-integrated x-ray emission from the extremely small spot size of the irradiated foil. The microscope was fitted with a 100-nm aluminum and 3.2-μm Mylar filter to examine x-ray energies of about 1 keV. The microscope viewed the rear of the target along the laser axis. Three Dante multichannel x-ray diode systems provided high-precision broadband intensity measurements.[5]

Target absorption was measured with an array of scattered-light pin diodes, filtered to record wavelengths of 1064 nm, and with incident and backscattered calorimeters. For the absorption measurements, the iron and iron-copper targets were oriented at normal incidence to facilitate angular integration over the finite pin-diode array. The

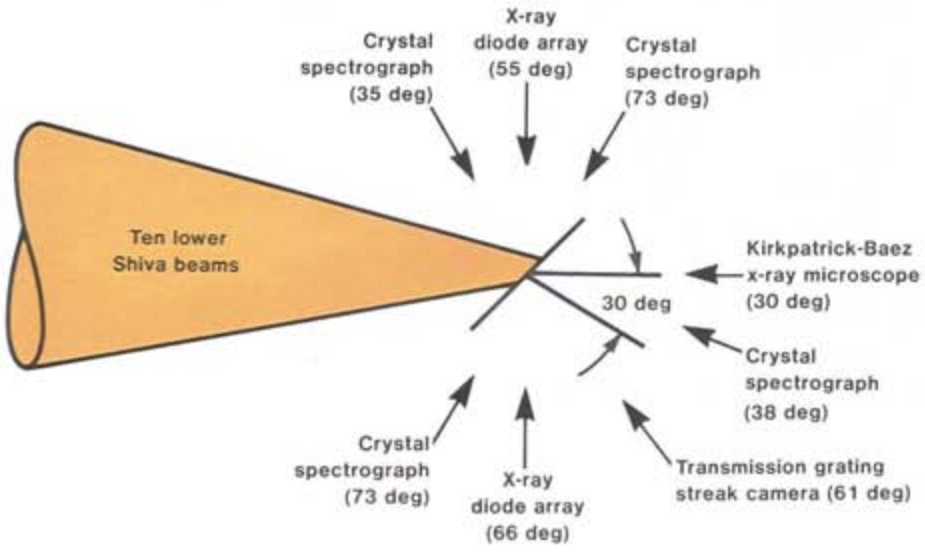

Fig. 4

Configuration of diagnostic instruments used in the Shiva x-ray experiments. To measure the x-ray spectrum emitted by the flashlamp target, two time- and space-integrated crystal spectrometers viewed it from the front (the surface irradiated by the laser light) and two from the rear. For aborption measurements, the target was irradiated normal to the beam axis. To enable the instruments to view it from both sides, the target was rotated 30 deg.

total energy, pulse length, and beam balance of the Shiva laser were also carefully monitored.

Experimental Results

The laser pulse widths were measured by three streak cameras and varied from 100 to 133 ps. Shiva's ten lower beams were overlapped to give a nominal spot diameter of 1 mm. Laser energies on target ranged from 142 to 374 J. Typical peak intensities of the incident laser light were 100 to 200 TW/cm^2.

Target Absorption

Because of the large effective f/number (f/1) of Shiva's beam clusters and the laser duration used (100 to 120 ps), the dependence of target absorption on the angle of incidence of the laser light should be negligible (at least for angles less than 30 deg). (This assumption is supported by experiments with the Laboratory's Argus laser where we used an enclosing box calorimeter to measure reflected and scattered laser light.) In addition, we do not expect absorption to depend significantly on the atomic number of the target material over the modest range covered in these experiments.

Two experiments gave laser-light absorption values of 50 ± 5% for an iron foil and 39 ± 4% for an iron/copper foil. These absorption values were inferred by subtracting the backscattered light and the integrated scattered light measurements from the incident laser energy. Measurement errors due to calibration uncertainties and angular integration give an average absorption value of 45 ± 9% for these two experiments.

Source Uniformity

We measured the two-dimensional, time-integrated spatial characteristics of the x-ray emission region with the Kirkpatrick-Baez microscope. The aluminum-Mylar filter resulted in a channel response of about 0.8 to 1.2 keV. Figure 5 shows a processed spatial image of a nickel-foil experiment. The relatively soft edge of the image may result from time integration

Calibrating the response of the film used in the spectrographs was a formidable task; it represents the least certain quantity in determining the absolute intensity of the x-ray lines emitted from the flashlamp foils.

and from overlapping of Shiva's ten beams. The image shows no small-scale structure (time integration may again be responsible), although there is a relatively long-scale variation (1.5:1) in the film density over a scale length of about 500 to 700 μm. We used this image to determine the area of the source in estimating the brightness of the x-ray flashlamp. (The brightness of the source is defined as the intensity radiated per unit time per unit photon energy interval.)

X-Ray Spectra

In our detailed measurements of the x-ray emission spectra, several quantities were of particular interest: the total yield and power of the x-ray emissions from the flashlamp, the angular dependence and relative strength of the spectral lines, and the energy and brightness of x-ray lines in the vicinity of the resonance with the upper energy level of the lasing medium. Total x-ray yield is an important quantity, as the flashlamp x rays serve to strip down the lasing gas to its helium- or hydrogen-like ionization state. The relative spectral emission strengths of transitions from various ionization states of the flashlamp foils, and their angular dependence on opacity effects, provided a valuable check on our simulation computer codes LASNEX and XRASER. Finally, the brightness of individual flashlamp emission lines is important because it determines both the possibility of creating a population inversion in the lasant gas as well as the laser gain.

To study these quantities, we combined measurements from several different instruments. Figure 6 shows typical time-integrated spectra obtained from chromium and nickel flashlamps with the transmission grating and streak camera; the spectra display strong L-shell emission. Although the instrument does not resolve individual lines, it does show that the energy centroid of emission increases with atomic number as expected. Figure 7 shows the time history of the

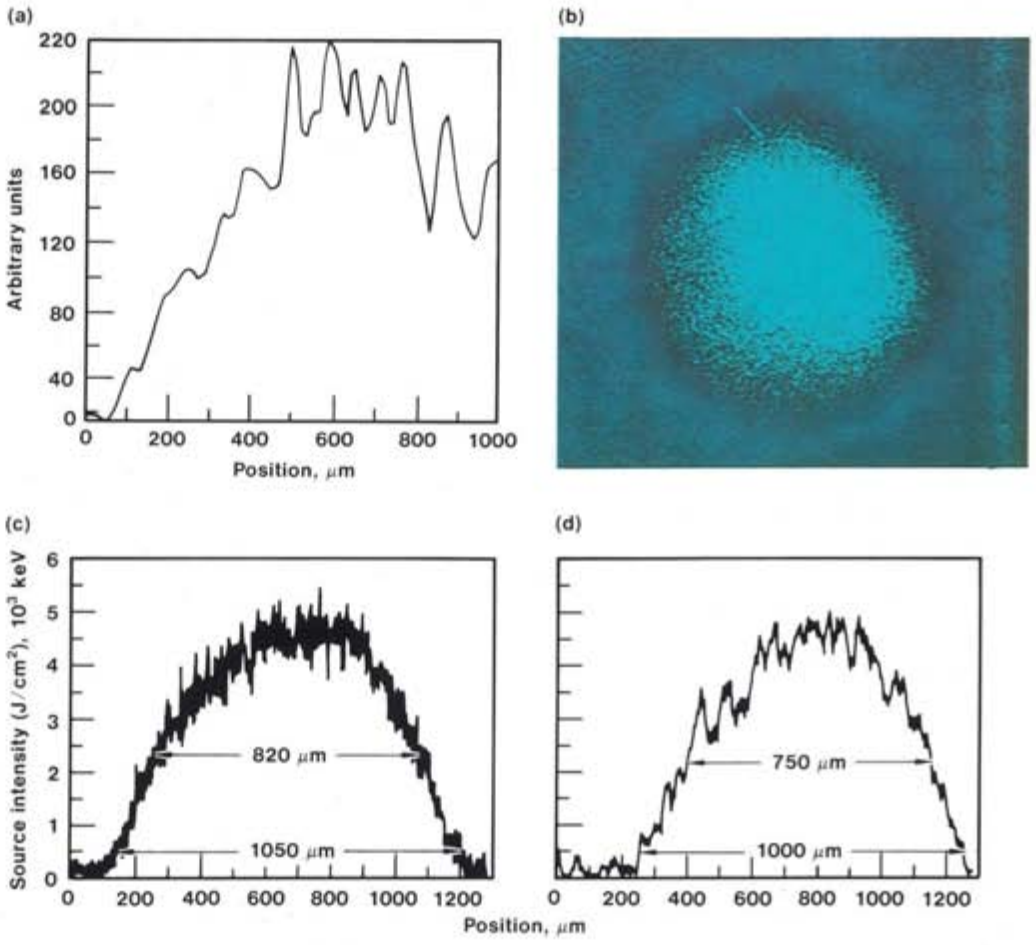

Fig. 5

(a) Spatial image of 1.064-μm light incident on the flashlamp foil. The scan represents the average optical density at the target plane. (b) Two-dimensional image of x rays emitted from flashlamp target in the energy interval from 0.8 to 1.2 keV. The spatial resolution of the x-ray microscope is about 10 μm. (c) Vertical scan through middle of the image, showing full-width half-maximum (FWHM) and full-width 0.1-maximum [FW(0.1)M] of the source intensity. (d) Horizontal scan through the middle of the image, showing FWHM and FW(0.1)M.

L-shell emission from a chromium flashlamp. The 100-ps rise time is consistent with a driving-laser pulse of 100 ps [the laser pulse is Gaussian, with a full-width half-maximum (FWHM) of 100 to 120 ps] but decays more slowly, with a characteristic time of about 220 ps. The FWHM of the x-ray emission is about 190 ps, 1.5 to 2 times greater than that of the laser pulse.

Chromium Spectrum

Figure 8a shows a typical time- and space-integrated spectrum obtained for chromium flashlamp foils using the 35-deg forward spectrograph (angle measured relative to target normal). Figure 8b shows the important case of a chromium spectrum obtained with the 38-deg rearward spectrograph. All data were energy calibrated with one of the lithium-like $n = 3 \rightarrow n = 2$ transitions. The spectral linewidths measured by the 35-deg forward and 38-deg rearward spectrographs were 1.8 and 1.4 eV FWHM, respectively. In both cases, the linewidth was dominated by source size. The smaller value resulted from a different instrument design located farther from the source.

The spectrum of chromium was one of the most important measured in the Shiva experiments because it is a prime candidate for pumping fluorine to produce a 42.3-eV x-ray laser. The beryllium-like chromium emission line necessary to pump the $n = 4$ level of helium-like fluorine was theoretically predicted to be 899.78 eV; this line was measured experimentally at 899.58 eV. The chromium emission record in Fig. 8b (from a rearward spectrograph) illustrates the uncertainty surrounding spectral calibrations. A distinct group of five lines from about 0.87 to 0.91 keV should be associated with beryllium-like $3d \rightarrow 2p$ transitions. Unfortunately, the uncertainty in our energy calibration ($\pm$ 4 eV) prevents any firm conclusions about whether the desired energy overlap occurs. Further measurements to improve the accuracy of these line determinations are in progress at KMS Fusion, Inc., Ann Arbor, Michigan; others will be performed at LLNL early in Novette's experimental schedule.

Line Brightness

To facilitate comparison with the kinetics calculated with the XRASER code, we have expressed the brightness of the flashlamp's pump line in terms of modal photon density (photons per mode). The modal photon density is a measure of a line's brightness at a given frequency, which can be compared to that of a blackbody radiating at a prescribed temperature. For an optically thick source in equilibrium, this

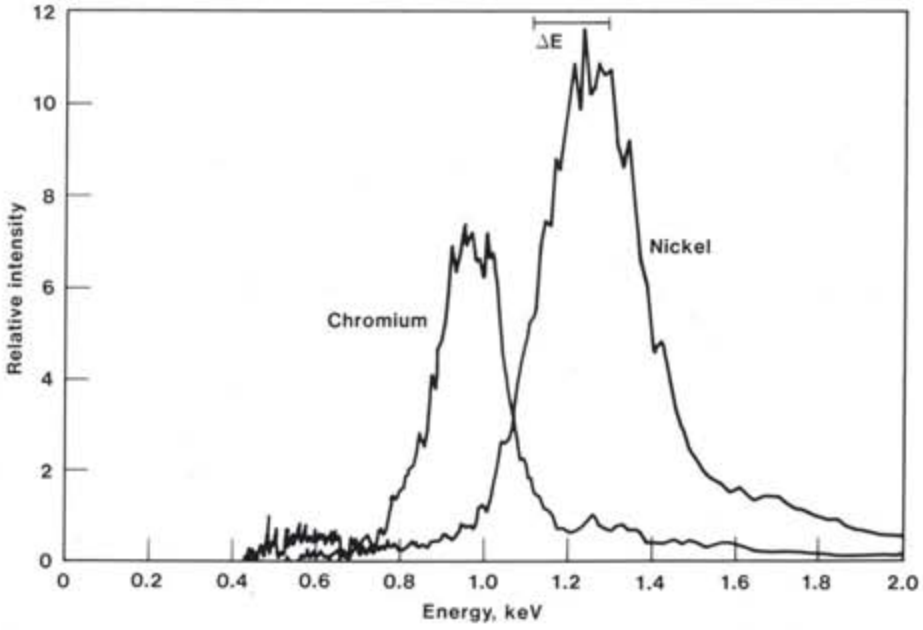

Fig. 6

X-ray spectrum produced by laser irradiation of chromium and nickel flashlamp foils. The interval ΔE (FWHM) indicates the resolution of the streaked transmission-grating spectrograph.

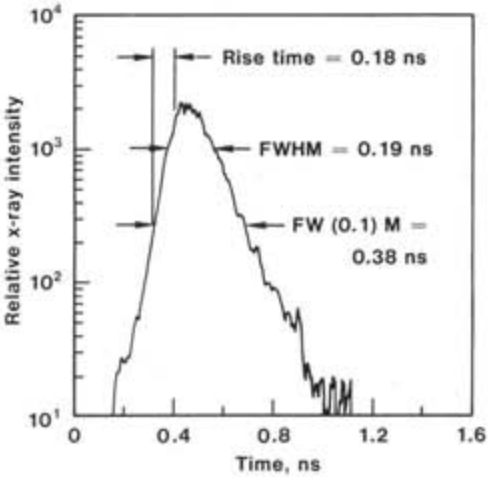

Fig. 7

Time history of x-ray emission at the peak intensity point in the chromium spectrum shown in Fig. 6.

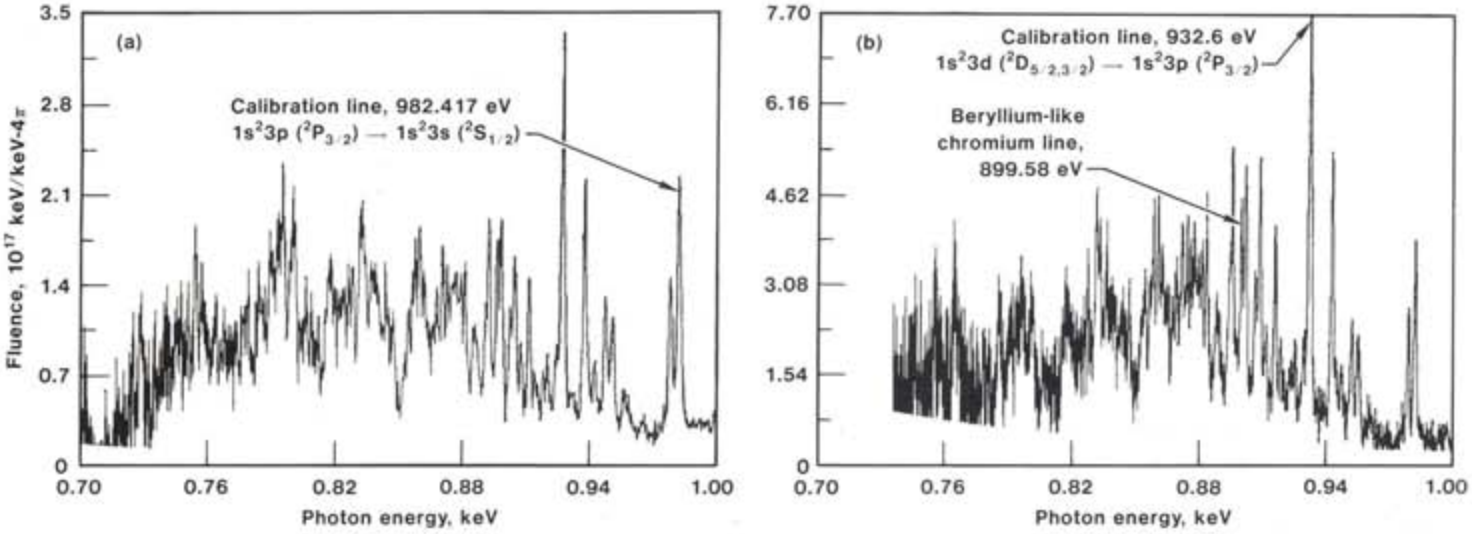

Fig. 8 (a) X-ray spectrum of the n = 3 → n = 2 emission from a chromium flashlamp foil, showing the calibration line; data obtained with the 35-deg forward crystal spectrograph. (b) X-ray spectrum of the n = 3 → n = 2 emission from the same chromium foil, showing the calibration line and one of the laser pump lines (beryllium-like chromium); data obtained with the 38-deg rearward spectrograph.

modal photon density is

$$N_p = [\exp(h\nu/kT) - 1]^{-1},$$

where h is Planck's constant, ν is the emission frequency, T is the temperature, and k is Boltzmann's constant. If $h\nu/kT = 1$, $N_p = 0.58$ photons per mode; if $h\nu/kT = 2.822$ (the peak of the blackbody spectrum), $N_p = 0.063$ photons per mode, and so on. In other words, N_p scales rapidly with kT when the photon energy is fixed, emphasizing the importance of heating the flashlamp to a relatively high electron temperature.

Table 2 Modal photon densities of the strongest lines in the flashlamp x-ray spectra for two different experiments.[a]

Flashlamp material	Spectral line	Line energy, eV	Photons/mode (forward 38-deg spectrograph)	Photons/mode (rearward 35-deg spectrograph)
Cr + CH	$1s^2 3d(^2D_{5/2}) — 1s^2 2p(^2P_{3/2})$	932.6	0.01	0.004
Cr + CH	$1s^2 3d(^2D_{5/2}) — 1s^2 2p(^2P_{3/2})$	932.6	0.009	0.005

[a]On the basis of the data from the x-ray microscope, we assumed an emission area of 6.4×10^{-3} cm². We obtained a value of $\Delta\tau$ from the transmission grating and streak camera on one experiment only; in others, it was assumed to be 200 ps. The instrument source-broadened linewidth was about 1.5 eV FWHM for the forward spectrograph and about 1.8 eV for the rearward spectrograph; the natural (Dopper-broadened) linewidth was assumed to be about 0.3 eV FWHM.

Most laser photoexcitation schemes require flashlamp photon densities of at least 0.01 photons per mode. The quantity N_p (photons per mode) is related to parameters we actually measure by

$$N_p = (2.56 \times 10^{-24})\, E_{h\nu}^{-3}\, \Delta\tau^{-1}\, A^{-1} \times I\, (\Delta E_{exp}/\Delta E_{natural}),$$

where $E_{h\nu}$ is the transition energy in electron volts, $\Delta\tau$ is the duration of the transition (FWHM) in seconds, A is the emission area of the plasma in square centimetres, I is the measured x-ray intensity in units of keV/keV over 4π, and $\Delta E_{exp}/\Delta E_{natural}$ is the ratio of the experimental linewidth (FWHM) to the natural (Doppler-broadened) linewidth. In our experiments, I is uncertain to within ± 50%. We did not measure the uncertainty in $\Delta\tau$ because the duration of emission was not determined for individual lines. The ratio $\Delta E_{exp}/\Delta E_{natural}$ is known to within ± 50%. These uncertainties lead to a large uncertainty in N_p. Future experiments at KMS Fusion and LLNL (with Novette) will focus on reducing the error in each of these parameters.

Table 2 shows some of the modal photon intensities derived for the most intense lines observed in the spectrum of the chromium-hydrocarbon flashlamp foil. (We used the transmission-grating streak camera to determine $\Delta\tau$.) The brightness of the lines assumed to be candidates for pumping the x-ray laser (from the beryllium-like state) was

about one half of the value (0.01 photons per mode) that appears necessary for photopumping the transitions of interest. Although the data embody considerable uncertainty, we will attempt to increase the value of N_p in the early phases of the Novette x-ray-laser experiments using techniques based on the wide range of irradiation conditions (a wavelength of 532 nm and higher intensities) that Novette will provide.

Summary

A popular scheme proposed for lasing at x-ray wavelengths is based on resonant photopumping of the lasing medium by x rays generated in laser-irradiated metal foils. To evaluate the quantitative feasibility of such schemes, we must first determine the x-ray emission characteristics of the foils. We used the Laboratory's Shiva laser to irradiate a number of candidate flashlamp materials. Our experiments established the feasibility of producing a bright, uniform source of x radiation in the range of wavelengths required. However, the experiments underscored uncertainties in several key parameters. To reduce the uncertainties, we will need to make more accurate determinations of the centroid energy and the width of flashlamp emission lines. We must also measure the time duration of individual emission lines with a high-resolution spectograph.

Our experience in these preliminary experiments with the Shiva laser will be applied to a much more accurate assessment of flashlamp line brightness using LLNL's Novette laser later this year. Because x-ray lasing would be marginal for some schemes at current line brightnesses, the Novette experiments will also explore techniques of increasing brightness by studying the effects of such parameters as the wavelength and intensity of the driving laser light and the thickness of the flashlamp foil.

Key Words: LASNEX; laser—Novette, Shiva, x-ray; XRASER.

Notes and References

1. A number of x-ray lasing schemes are described in P. L. Hagelstein, *Physics of Short Wavelength Laser Design*, Lawrence Livermore National Laboratory, Rept. UCRL-53100 (1981).
2. The experimental procedure and results for these spectrographs are described in M. Boyle and L. Koppel, *Crystal Spectrograph Measurements for Laser Produced X-Ray Wavelength Identification*, Advanced Research and Applications Corporation, Sunnyvale, California, Rept. TR-139-02 (1982).
3. R. L. Kaufmann, G. L. Stradling, D. T. Attwood, and H. Medecki, *Quantitative Intensity Measurements Using a Soft X-Ray Streak Camera*, Lawrence Livermore National Laboratory, Rept. UCRL-87963 (1982).
4. N. M. Ceglio, R. L. Kauffman, A. Hawryluk, and H. Medecki, *A Time-Resolved X-Ray Transmission Grating Spectrometer for Investigation of Laser-Produced Plasmas*, Lawrence Livermore National Laboratory, Rept. UCRL-87800 (1982).
5. For a discussion of new diagnostic instruments used in laser fusion x-ray experiments, see the article beginning on p. 13 of this issue of *Energy and Technology Review*.